Human Molecular Genetics, 2004, Vol. 13, No. 18 **2143–2153**
doi:10.1093/hmg/ddh218
Advance Access published on July 14, 2004

Transcription profiling of inner ears from *Pou4f3*$^{ddl/ddl}$ identifies Gfi1 as a target of the Pou4f3 deafness gene

Ronna Hertzano[1,2,7], Mireille Montcouquiol[2], Sharon Rashi-Elkeles[3], Rani Elkon[3], Raif Yücel[4], Wayne N. Frankel[5], Gideon Rechavi[6], Tarik Möröy[4], Thomas B. Friedman[7], Matthew W. Kelley[2] and Karen B. Avraham[1,*]

[1]Department of Human Genetics and Molecular Medicine, Sackler School of Medicine, Tel Aviv University, Tel Aviv 69978, Israel, [2]Section on Developmental Neuroscience, National Institute on Deafness and Other Communication Disorders, National Institutes of Health, Rockville, Maryland 20850, USA, [3]The David and Inez Myers Laboratory for Genetic Research, Department of Human Genetics and Molecular Medicine, Sackler School of Medicine, Tel Aviv University, Tel Aviv 69978, Israel, [4]Institut für Zellbiologie (Tumorforschung), Universitätsklinikum Essen, Virchowstrasse 173, D-45122 Essen, Germany, [5]The Jackson Laboratory, Bar Harbor, Maine 04609, USA, [6]Department of Pediatric Hemato-Oncology and Institute of Hematology, The Chaim Sheba Medical Center, Tel-Hashomer and Sackler School of Medicine, Tel Aviv University, Tel Aviv 52621, Israel and [7]Section on Human Genetics, Laboratory of Molecular Genetics, National Institute on Deafness and Other Communication Disorders, National Institutes of Health, Rockville, MD 20850, USA

Received June 2, 2004; Revised and Accepted July 2, 2004

Pou4f3 (Brn3.1, Brn3c) is a class IV POU domain transcription factor that has a central function in the development of all hair cells in the human and mouse inner ear sensory epithelia. A mutation of *POU4F3* underlies human autosomal dominant non-syndromic progressive hearing loss DFNA15. Through a comparison of inner ear gene expression profiles of E16.5 wild-type and *Pou4f3* mutant deaf mice using a high density oligonucleotide microarray, we identified the gene encoding growth factor independence 1 (*Gfi1*) as a likely *in vivo* target gene regulated by Pou4f3. To validate this result, we performed semi-quantitative RT–PCR and *in situ* hybridizations for *Gfi1* on wild-type and *Pou4f3* mutant mice. Our results demonstrate that a deficiency of *Pou4f3* leads to a statistically significant reduction in *Gfi1* expression levels and that the dynamics of *Gfi1* mRNA abundance closely follow the pattern of expression for *Pou4f3.* To examine the role of Gfi1 in the pathogenesis of Pou4f3-related deafness, we performed comparative analyses of the embryonic inner ears of *Pou4f3* and *Gfi1* mouse mutants using immunohistochemistry and scanning electron microscopy. The loss of *Gfi1* results in outer hair cell degeneration, which appears comparable to that observed in *Pou4f3* mutants. These results identify *Gfi1* as the first downstream target of a hair cell specific transcription factor and suggest that outer hair cell degeneration in *Pou4f3* mutants is largely or entirely a result of the loss of expression of *Gfi1*.

INTRODUCTION

Hearing loss is a common inherited sensory disorder, affecting ~1 in 2000 newborns and a significant portion of the elderly population (1). To date, mutations in 37 genes have been shown to result in human non-syndromic hearing loss (NSHL) (2,3) (see Hereditary Hearing Loss homepage, http://www.uia.ac.be/dnalab/hhh/). We previously reported a dominant mutation in the *POU4F3* transcription factor that causes a progressive form of NSHL, in an Israeli Jewish family (4,5). Similarly, mice that are homozygous for a recessive targeted knockout allele of *Pou4f3* (Brn3c/Brn3.1) are deaf and have a vestibular dysfunction due to loss of hair cells of the inner ear (6–8). Hair cells in the inner ear are cells with actin-rich apical projections named stereocilia, which function as mechanosensors and transducers of sound

*To whom correspondence should be addressed. Tel: +972 36407030; Fax: +972 36409360; Email: karena@post.tau.ac.il

 © *Oxford University Press 2004; all rights reserved*

and movement in the auditory and vestibular systems, respectively (9).

Mammalian class IV POU domain transcription factors (Pou4f1, Pou4f2 and Pou4f3), are each expressed in overlapping subsets of cells of neuronal origin and are essential for the differentiation and survival of that cell type (6,8,10–12). Pou4f3 is expressed in all hair cells of the inner ear as soon as they leave the cell cycle (13), between E12 and E15 (14). In the absence of Pou4f3, hair cells begin to form, but undergo apoptosis beginning at E17, resulting in a complete depletion of hair cells from all inner ear sensory epithelia by early postnatal stages (13,15). These data indicate that genes regulated by Pou4f3 are necessary for hair cell survival and differentiation but not for determination of cell fate. However, to date, no *in vivo* target genes of Pou4f3, or of other transcription factors implicated in hair cell development have been reported (16–18).

We sought to identify and validate the downstream *in vivo* target genes of Pou4f3 by comparing mRNA expression profiles from E16.5 inner ears of wild-type and *Pou4f3* homozygous mutant mice. We found that expression of *Gfi1* (growth factor independence 1), a zinc-finger transcription factor, is downregulated in the ears of the *Pou4f3* mutant mice. Mice with targeted mutations in *Gfi1* are deaf and have vestibular dysfunction due to hair cell loss, but also suffer from severe neutropenia and defects in T-cell differentiation (18–20). Our data indicate that reduced levels of Gfi1 appear to be responsible for the loss of outer hair cells in the cochlea of *Pou4f3* mutant mice.

RESULTS

The dreidel mouse mutant

Pou4f3$^{ddl/ddl}$ mice are deaf and exhibit vertical head tossing, circling and general hyperactive behavior indicative of a vestibular dysfunction. The dreidel (*ddl*) mutation arose on the C57BL/6J strain background, was subsequently mapped to chromosome 18 near the *Pou4f3* locus and was found to be a TG dinucleotide deletion (388del2) in the *Pou4f3* coding sequence, which is predicted to truncate this protein prior to the POU-specific DNA binding domain, rendering the transcription factor non-functional (data not shown). Auditory brainstem response (ABR) thresholds of deaf *Pou4f3*$^{ddl/ddl}$ mice were determined to be above 100 dB SPL (data not shown) whereas the ABR thresholds of age-matched C57BL/6J *Pou4f3*$^{ddl/+}$ mice were 35 dB SPL, which is indistinguishable from wild-type mice. A similar hearing loss phenotype was also reported for the *Pou4f3* knockout mice (*Pou4f3*$^{-/-}$) (6,8), suggesting that *Pou4f3*$^{ddl/ddl}$ mice are a second mouse model for a loss of function of Pou4f3.

Expression profiling of embryonic mouse inner ears

To identify downstream *in vivo* target genes of Pou4f3 we examined global gene expression profiles of whole inner ears from E16.5 *Pou4f3*$^{ddl/ddl}$ and their wild-type littermates, using the Affymetrix Murine Genome U74Av2 oligonucleotide microarrays (Supplementary Material, Table S1). We chose E16.5 because by this time point Pou4f3 is already expressed in most of the hair cells of the inner ear, and hair cell degeneration is still minimal (13). In the mouse inner ear, hair cells consist of $<1\%$ of the total number of cells, yet expression of hair cell specific genes (e.g. *Myo6*, *Myo7a* and *Clcn3*) was readily detected, notwithstanding their minor contribution to the total RNA pool (21). For a comparison of our microarray results with online databases of gene expression in the inner ear, see Supplementary Material.

Gfi1 mRNA levels are decreased in the *Pou4f3* mutant inner ears

We found *Gfi1* to be downregulated in the RNA samples from *Pou4f3*$^{ddl/ddl}$ inner ears when compared with the RNA samples from their wild-type littermate controls, confirmed by a *t*-test analysis (Supplementary Material, Table S1). Moreover, *Gfi1* was identified as 'absent' in all five replicas of the *Pou4f3*$^{ddl/ddl}$ samples in our microarray experiments while being identified as 'present' in all six hybridizations from the wild-type littermates. In order to validate these results, we quantified the mRNA abundance of *Gfi1* in the inner ears of wild-type and *Pou4f3*$^{ddl/ddl}$ homozygote mutant mice at E16 and E18.5. To control for potential non-specific decreases in mRNA expression as a result of hair cell death, the relative abundances of mRNAs for the hair cell specific genes *Pou4f3*, myosin VI (*Myo6*) and myosin VIIa (*Myo7a*) were also determined.

Real-time semi-quantitative RT–PCR results from both E16 and E18.5 inner ears indicate that the level of expression for *Myo6*, *Myo7a* and *Pou4f3* in *Pou4f3*$^{ddl/ddl}$ mice is $\sim$63–88% of the level of expression of age-matched wild-type mice (Fig. 1A–C). This decrease is probably the result of ongoing hair cell degeneration and loss. In contrast to myosin VI and myosin VIIa, expression of *Gfi1* in *Pou4f3*$^{ddl/ddl}$ mice is decreased to 5–8% of the mRNA abundance found in wild-type controls ($P < 0.001$) (Fig. 1D), suggesting that the decrease in *Gfi1* is a result of the absence of Pou4f3, and not just owing to general hair cell loss. Furthermore, the quantification of *Myo6*, *Myo7a* and *Gfi1* mRNA abundance was repeated with RNA extracted at comparable time points from ears of *Pou4f3*$^{-/-}$ mice. Results (data not shown) were similar to those of *Pou4f3*$^{ddl/ddl}$ (Fig. 1A–D).

The expression of *Gfi1* follows the pattern of *Pou4f3* in the developing organ of Corti

Total RNA was isolated at seven time points between E12 and P3 from cochlear sensory epithelia that had been isolated from the surrounding mesenchyme and other cell types (22). The dynamics of *Pou4f3* and *Gfi1* mRNA abundance in the developing auditory sensory epithelium were determined by semi-quantitative RT–PCR. Very low levels of *Pou4f3* mRNA were detected at developmental stages E12 and E13.5, and their abundance increased consistently at later developmental time points (Fig. 1E). *Gfi1* expression was first detected at E15.5, and thereafter followed an expression pattern similar to that seen for *Pou4f3* (Fig. 1F). This is consistent with previously published data, showing that while *Gfi1* mRNA can be detected at E12.5 in the otocyst, *Gfi1* expression in the organ of Corti is limited to the hair cells (18, this manuscript). In

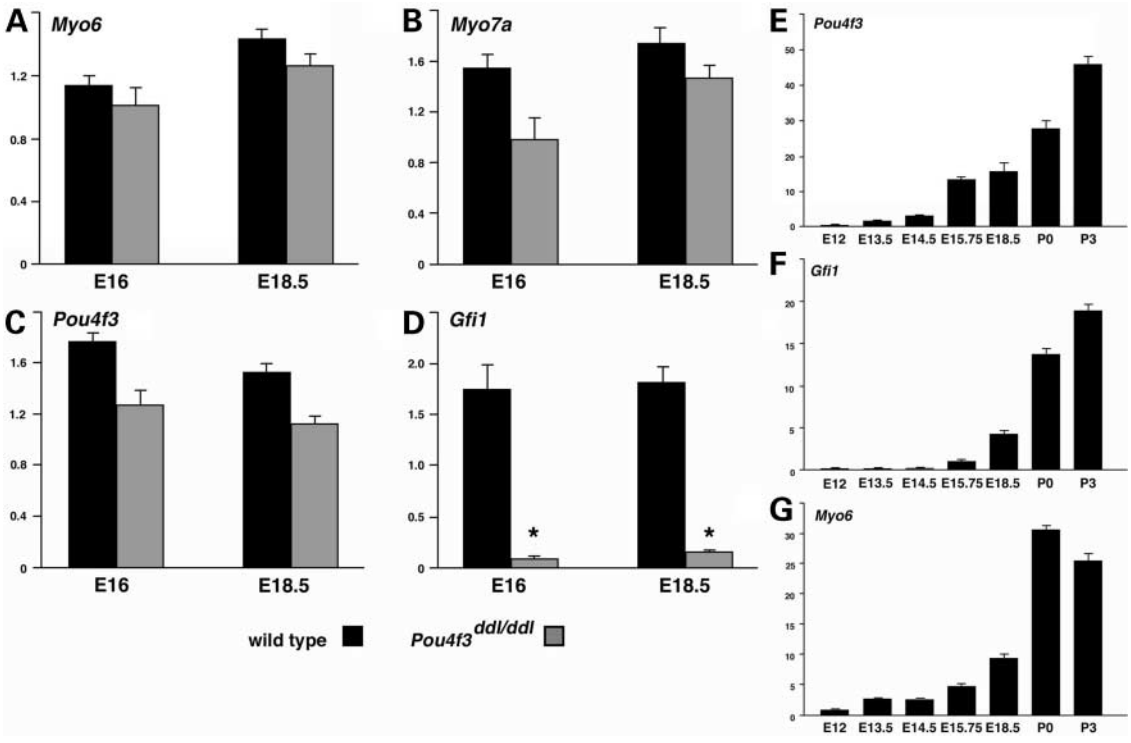

Figure 1. *Gfi1* mRNA is specifically downregulated in the ears of E16 and E18.5 *Pou4f3*$^{ddl/ddl}$ mice and follows the developmental quantitative expression of *Pou4f3* in the developing organ of Corti. The first four bar diagrams represent the relative abundance of *Myo6* (**A**), *Myo7a* (**B**), *Pou4f3* (**C**) and *Gfi1* (**D**) mRNA transcripts in the ears of wild-type (black bars) and *Pou4f3*$^{ddl/ddl}$ (gray bars) mice. The three hair cell specific genes, *Myo6*, *Myo7a* and *Pou4f3*, exhibit a small, not statistically significant, reduction of mRNA expression in *Pou4f3*$^{ddl/ddl}$ at both E16.5 and E18.5 compared with wild-type. This small difference is consistent with ongoing hair cell death within the inner ear epithelia. In contrast, *Gfi1* mRNA is dramatically reduced in *Pou4f3*$^{ddl/ddl}$, and reaches only 5–8% of the mRNA abundance found in wild-type controls ($P < 0.001$). Next, *Pou4f3* (**E**), *Gfi1* (**F**) and *Myo6* (**G**) mRNA abundances were determined by semi-quantitative RT–PCR on cDNA extracted from thermolysin treated cochlear epithelia at seven developmental time points. Small amounts of *Pou4f3* mRNA can be detected as early as E12, and their levels constantly increase until P3, the latest stage analyzed (E). *Gfi1* mRNA follows a similar pattern, but it could only begin to be detected at E15.5, a delay consistent with Pou4f3 regulating its expression. *Y*-axis: mRNA, arbitrary units; *X*-axis: developmental time points. An asterisk indicates a significant difference between wild-type and mutant mRNA transcript abundance ($P < 0.001$). Error bars represent one standard error, $N = 6$ (A–D), $N = 3$ (E–G).

contrast, *Myo6* mRNA showed a different expression pattern. *Myo6* mRNA was detected as early as E12 and showed a decreasing level of expression between P0 and P3 (Fig. 1G), indicating that individual hair cell specific genes can have different patterns of mRNA abundance.

Gfi1 mRNA is expressed in hair cells of wild-type mice but absent in *Pou4f3* mutants

Next, we examined the expression of *Pou4f3* and *Gfi1* mRNA in cochlear and vestibular epithelia of E18.5 wild-type and *Pou4f3*$^{ddl/ddl}$ homozygous mutant mice by *in situ* hybridization using digoxigenin labeled sense and antisense probes. Both *Pou4f3* and *Gfi1* mRNAs were detected in a band that extended along the length of the cochlea, consistent with the position of the inner and outer hair cells (Fig. 2A and C). To study the expression of *Gfi1* in inner ear hair cells *in vivo*, we used a reporter mouse line in which part of the *Gfi1* coding region had been replaced by cDNA encoding green fluorescent protein (GFP) (23). Immunohistochemistry of the Gfi1:GFP knock-in mice inner ears at E18.5 indicated that Gfi1 is expressed specifically in the hair cells of all auditory and vestibular epithelia, confirming the published data and our *in situ* hybridization results (18) (Supplementary Material, Fig. S1). However, whereas mutant *Pou4f3* mRNA was expressed in *Pou4f3*$^{ddl/ddl}$ mice in a pattern similar to wild-type, *Gfi1* mRNA was not detected in any of the inner ear sensory epithelia examined (Fig. 2B and D). These results are consistent with regulation of *Gfi1* by Pou4f3, and indicate that even though hair cells are present in the cochleae of *Pou4f3*$^{ddl/ddl}$ at E18.5, functional Pou4f3 protein is required for the expression of *Gfi1* mRNA within these cells.

Math1 and Pou4f3 expression in the ears of *Pou4f3* and *Gfi1* mutants

Math1 is essential for hair cell development (16). It has been previously shown that Math1 acts upstream of *Gfi1* and that *Math1* is expressed in the ears of the *Gfi1* mutant mice (18). To test whether *Math1* is expressed in the inner ears of *Pou4f3*$^{ddl/ddl}$ mice, we performed real-time semi-quantitative RT–PCR. Our data indicate that at E16 and E18.5 *Math1* expression in inner ears from *Pou4f3*$^{ddl/ddl}$ mice is ~50% of the level of expression in the inner ears of wild-type mice (data not shown), suggesting that Pou4f3 might participate in the maintenance of *Math1* expression. This result, together

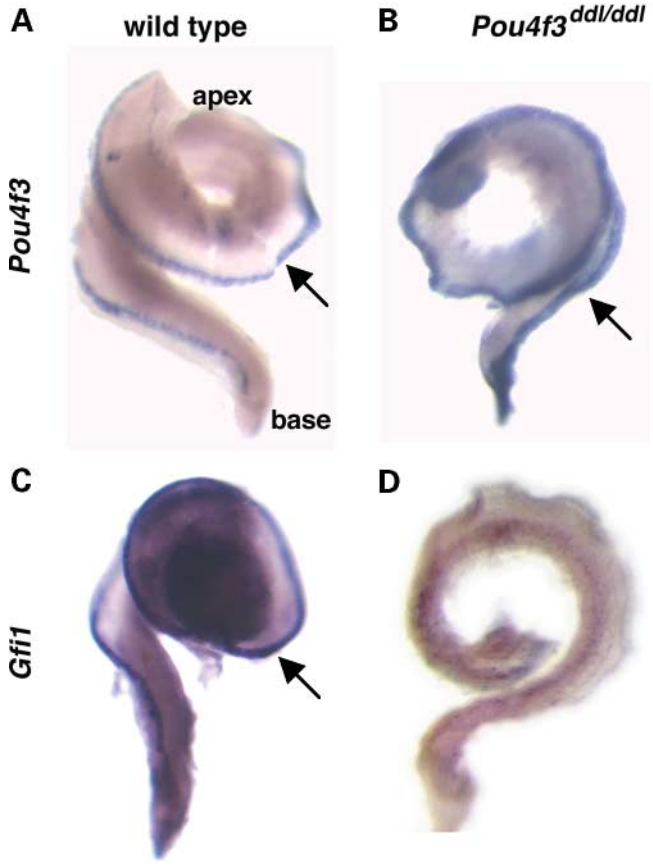

Figure 2. *Gfi1* mRNA is not detected in the E18.5 cochlea of *Pou4f3*$^{ddl/ddl}$ mice. Whole mount *in situ* hybridization was performed on E18.5 cochlea from *Pou4f3*$^{ddl/ddl}$ (**B**, **D**) and their wild-type littermate controls (**A**, **C**) using digoxigenin labeled antisense probes for *Pou4f3* (A, B) and *Gfi1* (C, D). *Pou4f3* and *Gfi1* mRNAs were detected as purple bands along the lateral border of the cochlea in a position that was consistent with inner and outer hair cells in both wild-type and mutant mice (arrows); *Gfi1* mRNA was not detected in the cochlea of the *Pou4f3* mutant mice. This experiment was repeated on consecutive sections of *Pou4f3*$^{ddl/ddl}$ and wild-type inner ears with similar results (data not shown).

with the wild-type hair cell phenotype of the *Math1*$^{+/-}$ mice, suggests that the decrease in levels of *Gfi1* expression in the ears of the *Pou4f3* mutant mice is not a result of an absence of *Math1* (16). To confirm that Pou4f3 is expressed in cochleae in the absence of Gfi1, we performed immunohistochemistry with the antibody for Pou4f3 on ears of E19.5 *Gfi1* mutant mice that have been described earlier (20). Both *Pou4f3* mRNA and protein are expressed in the ears of the E18.5, and E19.5 *Gfi1*$^{-/-}$ mice, respectively (18; Supplementary Material, Fig. S2).

Outer hair cells of *Pou4f3* and *Gfi1* mutants have similar phenotypes

Though the *Pou4f3* knockout mice have been previously characterized, an analysis of the progression of hair cell loss, hair cell surface morphology and supporting cells fate was not performed in the embryonic *Pou4f3* mutant auditory epithelium. Therefore, to determine whether loss of *Gfi1* can account for some of the defects observed in the *Pou4f3* mutant mice, cochleae were assessed by immunohistochemistry with an antibody for myosin VI or reacted with an antibody against p75^{ntr}, which labels pillar and Hensen cells (24), and with phalloidin, which labels filamentous actin. In wild-type cochleae, the sensory epithelium is organized in a mosaic pattern of supporting cells and myosin VI-positive inner and outer hair cells. The supporting cells include two rows of pillar cells located between the inner and first row of outer hair cells, Hensen's cells lateral to the third row of outer hair cells as well as Deiter cells, and phalangeal cells (Fig. 3A–D; data not shown). Outer hair cell morphology and patterning was markedly abnormal in the *Pou4f3*$^{-/-}$, *Pou4f3*$^{ddl/ddl}$ and *Gfi1*$^{-/-}$ mice. The three rows of outer hair cells were severely disrupted, and intact stereociliary bundles could not be identified with the phalloidin staining (Fig. 3E, F, I, J, M and N). Due to the disruption of hair cell morphology, individual cells were not readily distinguished with myosin VI staining (Fig. 3G, H, K, L, O and P). This effect was more pronounced in the basal region of the cochleae (Fig. 3H, L and P). The pattern of expression of myosin VI that we observed in these three mutants is consistent with substantial degeneration of the outer hair cells, suggesting that loss of *Gfi1* or *Pou4f3* is associated with a similar death of outer hair cells.

Although the outer hair cell phenotype was similar, there was a clear difference in the morphology of inner hair cells in cochleae from *Pou4f3*$^{-/-}$ and *Pou4f3*$^{ddl/ddl}$, when compared with cochleae from *Gfi1*$^{-/-}$ mice. In the apex of cochleae from *Pou4f3*$^{-/-}$ and *Pou4f3*$^{ddl/ddl}$ mice, inner hair cells were easily identified with the myosin VI staining but were clearly absent from the most basal 30–35% of the duct (Fig. 3G, H, K and L). In contrast, in *Gfi1*$^{-/-}$ mice inner hair cells were present along the entire length of the cochlea and were easily identified on the basis of the myosin VI and phalloidin staining (Fig. 3M–P). Similar, but less severe phenotypes of inner and outer hair cell degeneration were observed as early as E16.5 in cochleae from *Pou4f3*$^{-/-}$, *Pou4f3*$^{ddl/ddl}$ and *Gfi1*$^{-/-}$ mice (data not shown).

The p75^{ntr} staining was continuous at the apex of the wild-type, *Pou4f3*$^{dd/ddl}$, *Pou4f3*$^{-/-}$ and *Gfi1*$^{-/-}$, indicating that a row of pillar cells is clearly present (Fig. 3A, E, I and M). Interestingly, at the base of the *Pou4f3*$^{ddl/ddl}$ and *Pou4f3*$^{-/-}$ this staining was occasionally disrupted, suggesting a slow degeneration of the pillar cells that occurs in a wave that begins from the base of the cochlea toward the apex (Fig. 3F and J; arrows). In contrast with the base of the *Pou4f3*$^{ddl/ddl}$ and *Pou4f3*$^{-/-}$ cochleae, a line of undisrupted p75^{ntr} labeled cells was present in the basal regions of *Gfi1*$^{-/-}$ cochleae (Fig. 3N). This result, in addition to the presence of inner hair cells in the base of *Gfi1*$^{-/-}$ cochleae, and the difference in the p75^{ntr} staining between the base and the apex of the *Pou4f3* mutants, suggests a correlation between pillar cell survival and the presence of inner hair cells.

Inner and outer hair cell stereocilia bundles of *Pou4f3* and *Gfi1* mutants are disrupted

SEM was used to compare the surface morphology of cochlea from wild-type, *Pou4f3*$^{-/-}$ and *Gfi1*$^{-/-}$ mice at E18.5 and P0.

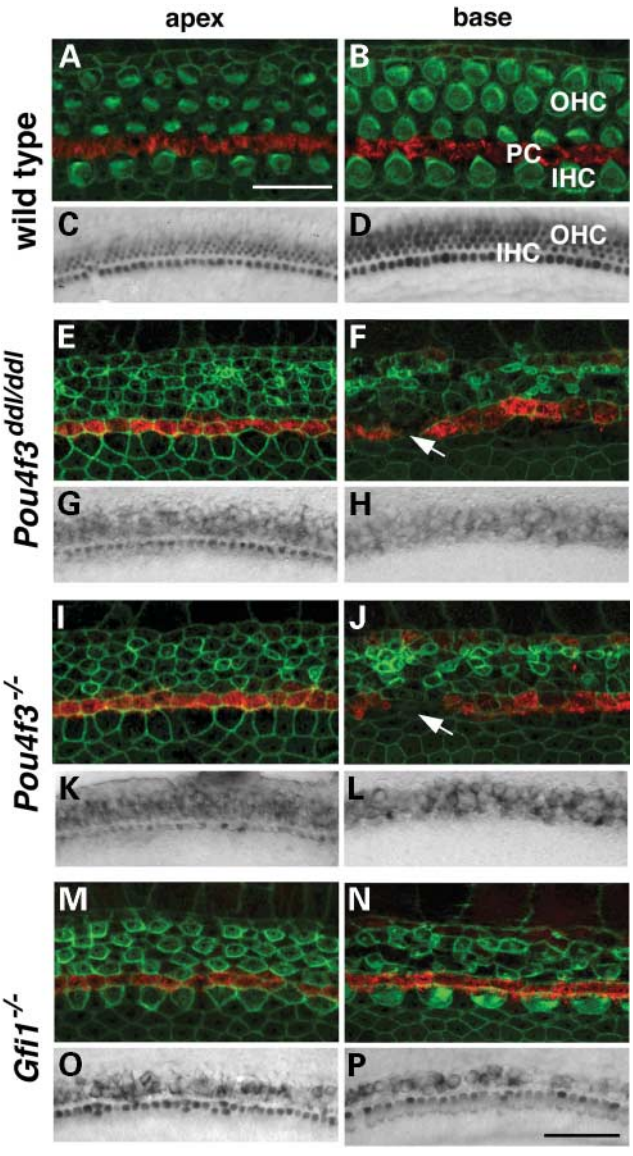

Figure 3. *Pou4f3* and *Gfi1* mutants exhibit similar phenotypes of degeneration of the outer hair cells. Top view of E18.5 whole mount cochleae from wild-type (**A**–**D**), $Pou4f3^{ddl/ddl}$ (**E**–**H**), $Pou4f3^{-/-}$ (**I**–**L**) and $Gfi1^{-/-}$ mice (**M**–**P**). The cochleae were stained with an antibody for $p75^{ntr}$ (red) that labels pillar and Hensen cells, and with phalloidin (green) to label filamentous actin at cell boundaries and in stereociliary bundles (A, B, E, F, I, J, M, N). Cochleae were also stained with an antibody for myosin VI (C, D, G, H, K, L, O, P). Similar patterning defects and hair cell degeneration of the outer hair region were observed in the base and the apex of the $Pou4f3^{-/-}$, $Pou4f3^{ddl/ddl}$ and $Gfi1^{-/-}$ cochleae, including the absence of well formed and differentiated hair bundles when compared with wild-type cochleae (E–P). However, at the base, inner hair cells can be detected only in the wild-type and $Gfi1^{-/-}$ mice (B, D, N, P) whereas no inner hair cells can be detected with the phalloidin staining or stain for myosin VI in the base of the *Pou4f3* mutant mice (F, H, J, L). In wild-type cochleae, a row of pillar cells heads (red) separating inner and outer hair cells is clearly present and continues undisrupted from base to apex (A, B). In the apex of the $Pou4f3^{-/-}$, $Pou4f3^{ddl/ddl}$ and $Gfi1^{-/-}$ mice, pillar cell staining appeared similar to the wild-type (E, I, M). In contrast, in the base of the $Pou4f3^{-/-}$ and $Pou4f3^{ddl/ddl}$ mutants, the pillar cell row appeared disrupted (F, J and arrows), suggesting that some pillar cells are missing. In the *Gfi1* mutants, the pillar cell row was undisrupted (N). OHC, outer hair cells; IHC, inner hair cells; PC, pillar cells. Scale bar: 10 μM (A, B, E, F, I, J, M, N); 50 μM (C, D, G, H, K, L, O, P).

In wild-type cochleae, the typical pattern of three rows of outer hair cells and one row of inner hair cells was present (Fig. 4A and B). The stereocilia in the apex of the wild-type cochlea were less mature (Fig. 4A), consistent with the basal to apical gradient in cochlear maturation (25,26). In the apical region of the cochleae of $Pou4f3^{-/-}$ mice, very small inner hair cells with poor luminal surface differentiation were observed, including an apparent absence of stereocilia. The outer hair cell arrangement was also disrupted, making it difficult to identify single hair cells. In the base, it was not possible to identify inner hair cells, whereas the outer hair cells luminal surface consisted of a sheath of poorly differentiated and disorganized apical projections and undistinguishable cell boundaries (Fig. 4C and D). In agreement with the cellular morphology analysis with myosin VI antibody (Fig. 3O and P), inner hair cells could be clearly identified both at the base and the apex of E18.5 $Gfi1^{-/-}$ mice cochlea, but appeared smaller and more immature when compared with wild-type inner hair cells. Apical extensions, probably primordia of stereociliary bundles, seemed shorter and less organized. The luminal surface of the outer hair cells throughout the length of the cochlea appeared very similar to the surface of the outer hair cells in the $Pou4f3^{-/-}$ mice (Fig. 4E and F).

Interestingly, a careful analysis of the base of the P0 $Pou4f3^{ddl/ddl}$ and $Pou4f3^{-/-}$ inner ears revealed that most of the epithelia had already degenerated (Fig. 4H). Long and aberrant stereocilia-like structures could be identified on the surface of some of these dying cells (Fig. 4I and J; data not shown). This observation is in contrast to previous reports indicating that stereocilia do not form in *Pou4f3* deficient mice (6,13).

STAT3, a downstream effector protein of Gfi1, localizes to the outer hair cells in the developing cochlear sensory epithelium

In order to address the differences in phenotype between the inner and outer hair cells in the *Gfi1* mutant mice, we chose to study the cochlear localization of bona fide downstream effector molecules of Gfi1 from the immune system. In T-cells, Gfi1 has been shown to increase signaling through STAT3 (signal transducer and activator of transcription 3) by binding to one of its inhibitors PIAS3 (protein inhibitor of activated STAT3) (27). As both STAT3 and PIAS3 were detected to be present in the microarray hybridization (Supplementary Material, Table S1), we performed immunohistochemistry with an antibody for STAT3 on cochleae from E16 and P0 wild-type mice (Fig. 5). STAT3 expression is localized mainly to the outer hair cells at both time points. Interestingly, at E16, the expression of STAT3 was mainly nuclear (Fig. 5A), whereas at P0 it was both nuclear and cytoplasmic (Fig. 5B–D).

DISCUSSION

Pou4f3 has a crucial role in the development and survival of hair cells in the mouse auditory and vestibular sensory epithelia. We used Affymetrix oligonucleotide microarrays to

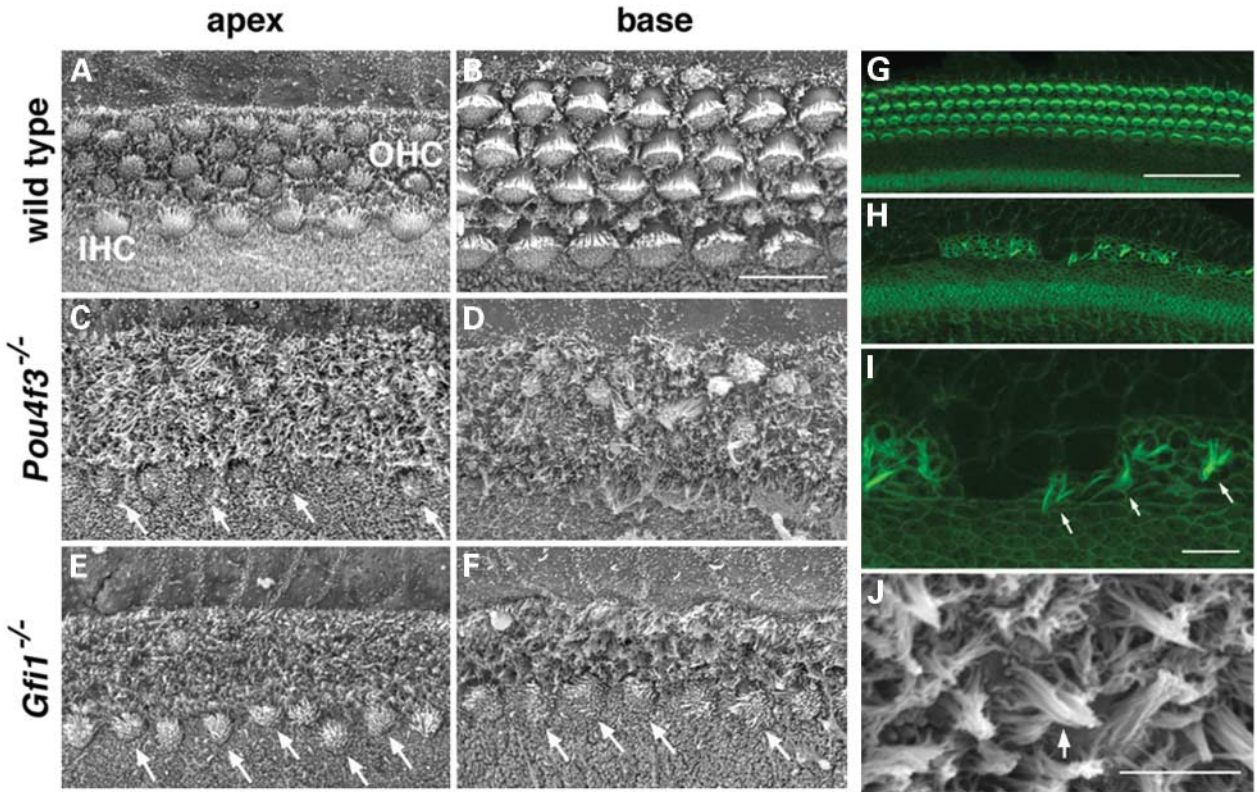

Figure 4. Surface morphology of cochlea from wild-type, *Pou4f3*$^{-/-}$ and *Gfi1*$^{-/-}$ mice at E18.5 and wild-type, *Pou4f3*$^{ddl/ddl}$ and *Pou4f3*$^{-/-}$ at P0. Scanning electron microscopy showing a surface view of the apical (**A**, **C**, **E**) and basal (**B**, **D**, **F**) parts of cochleae from E18.5 wild-type (A, B), *Pou4f3*$^{-/-}$ (C, D) and *Gfi1*$^{-/-}$ (E, F) mice. In wild-type cochlea, three rows of outer hair cells (top three rows) and one row of inner hair cells (bottom row) are clearly visible both at the apex and the base (A, B). In contrast, in cochlea from both *Pou4f3*$^{-/-}$ and *Gfi1*$^{-/-}$ mice, outer hair arrangement and surface morphology are disrupted making it difficult to identify single hair cells both at the base and the apex (C–F). However, while smaller and immature inner hair cells can be easily identified in the cochlea from the *Gfi1*$^{-/-}$ mice (E, F and arrows) when compared with wild-type cochleae, the inner hair cells seemed even smaller in the apical part of *Pou4f3*$^{-/-}$ mice (arrows), and could not be detected at the base (C, D). Top views of the basal parts of P0 whole mount cochleae stained with phalloidin (green) (**G**–**I**) from wild-type (G) and *Pou4f3*$^{ddl/ddl}$ (H, I) mice, and high magnification of a scanning electron micrograph of the remaining of an epithelial patch at the base of a *Pou4f3*$^{-/-}$ mouse (**J**). In the wild-type cochlea, the hair cells form three continuous lines of outer hair cells and one line of inner hair cells (G). In the *Pou4f3*$^{ddl/ddl}$ mice, most of the epithelium has degenerated, inner hair cells can not be identified and long and aberrant stereociliary-like structures can be identified on the surface of what could be the outer hair cell region (H, I and arrows). Similar stereociliary-like structures can also be identified in the scanning electron micrograph of such a sensory patch in the base of the *Pou4f3*$^{-/-}$ mice (J and arrow). Scale bar: 10 μM (A–F, I); 50 μM (G, H); 5 μM (J).

generate expression profiles of inner ears of *Pou4f3*$^{ddl/ddl}$ mutant and wild-type mice, and identified *Gfi1* as the first downstream target of an inner ear hair cell specific transcription factor.

Outer hair cell loss in *Pou4f3* and *Gfi1* mutants

Our analysis of both *Pou4f3* and *Gfi1* mutants demonstrates that outer hair cell morphology and degeneration is similar in both mutants. These results suggest that the phenotype of the outer hair cells in the *Pou4f3* mutants largely results from the loss of expression of Gfi1. In contrast, the inner hair cell phenotypes of these two mutants were different. Moreover, hair cells in the vestibular epithelia degenerate at a slower pace in the *Gfi1* mutant mice when compared to *Pou4f3* mutant mice (13,18). The inner hair cells and the vestibular hair cells may depend on survival and/or differentiation molecules other than Gfi1 that are downstream of Pou4f3. Gfi1 has also been found to enhance STAT3 signaling by binding to its inhibitor PIAS3 (27). STAT3 signaling has been shown to promote survival of sensory neurons (28) and can induce transcription of Bcl-2 family proteins such as Bcl-2 and Bcl-xL (29,30). As our results indicate that STAT3 is expressed in outer hair cells, it is possible that Gfi1 functions to promote hair cell survival by interacting with PIAS3 in the hair cells of the inner ear, thereby amplifying signals mediated through STAT3.

Although the pattern of outer hair cell death was very similar in the *Gfi1* and *Pou4f3* mutants, stereocilia were not distinguishable on the luminal surface of the outer hair cells of the *Gfi1* mutant mice at either E18.5 or P0. Conversely, long and aberrant stereocilia were clearly present on the apical surfaces of outer hair cells in *Pou4f3* mutants at both time points. The differences in the presence of inner and outer hair cells as well as in the surface morphology of some of the dying cells can probably be attributed to the abnormal regulation of other Pou4f3 downstream target genes that are yet to be identified and are independent of the Pou4f3–Gfi1 pathway. The striking difference in the phenotype of the inner hair cells of the *Pou4f3* and *Gfi1* mutant mice could be used for the identification of potential inner hair cell specific markers or survival molecules.

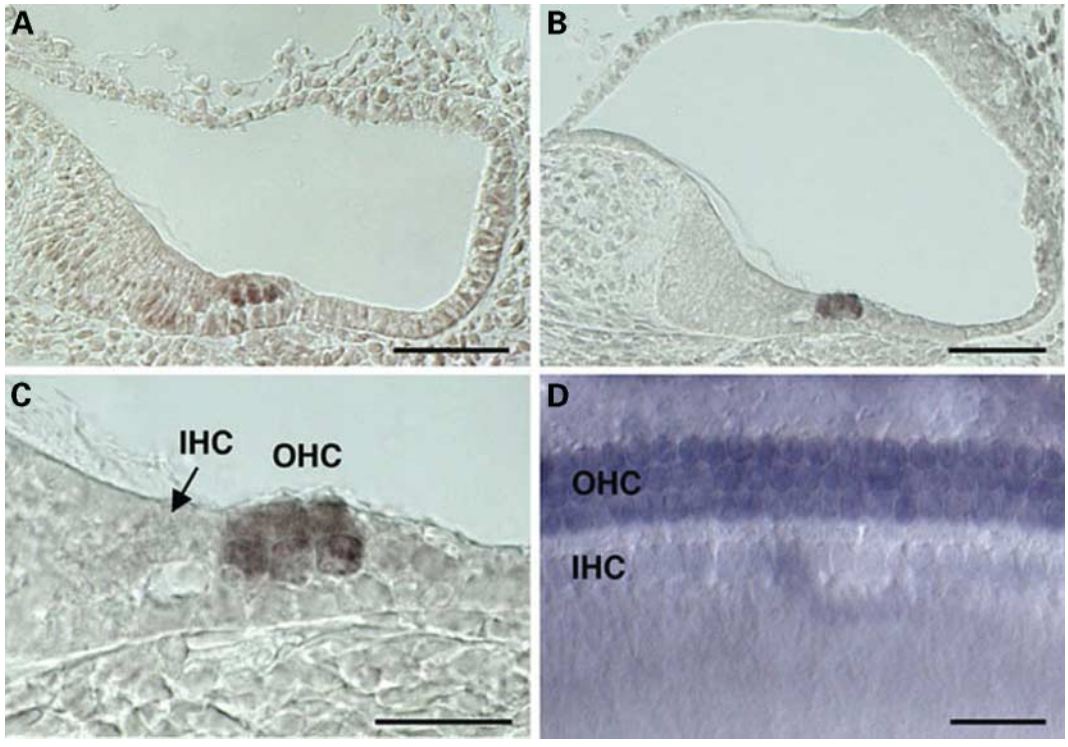

Figure 5. STAT3 expression is mainly localized to the outer hair cells in the developing organ of Corti. Immunocytochemistry with an antibody for STAT3 on cochlear sections from inner ears of E16 (**A**) and P0 (**B**, **C**) wild-type mice and on a whole mount of a cochlea from a P0 wild-type mouse (**D**). At E16, STAT3 expression is localized mainly to the nuclei of the outer hair cells. At P0, STAT3 expression is localized both in the nuclei and the cytoplasm of the outer hair cells (B–D). OHC, outer hair cells; IHC, inner hair cells. Scale bars: 50 μM (A, B); 25 μM (C, D).

The role of Gfi1 in the inner ear

Gfi1 is a nuclear zinc finger transcription factor that is able to function as a repressor of transcription via the SNAG N-terminal domain (SNAIL/Gfi1) that is conserved among the vertebrate members of the SNAIL/SLUG/Gfi1 family (31,32). Recent data point to an association of Gfi1 with the nuclear matrix, the co-repressor ETO as well as with histone deacetylases 1, 2 and 3 (HDAC-1, 2 and 3), which are chromatin modifying enzymes that function to close chromatin and silence transcription (33).

Gfi1 functions as a proto-oncoprotein regulating cell cycle control genes and functions to promote cell proliferation and prevent apoptosis (34–37). Additional potential effectors of Gfi1 in T-cells have been described and include c-Maf, LKLF, TRAF5 and the helix–loop–helix proteins inhibitors of differentiation and DNA binding 1 and 2 (Id1 and Id2) (38). This is of interest, as both Id1 and Id2 are expressed in the developing epithelium of the otic vesicle and the thickened epithelium of the developing cochlear duct (39), and can bind to basic helix–loop–helix transcription factors, such as Math1, preventing them from dimerizing and binding to DNA (reviewed in 40). Therefore, Gfi1 may contribute to the maintenance of Math1 expression at late embryonic stages by repressing Id1 expression (J. Jones and M.W. Kelley, unpublished data). In agreement with this hypothesis, Senseless (*Sense*), the *Drosophila* homolog of Gfi1, is required for cell maintenance and survival in the sensory organ precursor cells (SOP) that are dependent on the expression of proneural genes, including atonal, the Math1 homolog (41,42).

Conserved transcriptional cascades

In the nematode *Caenorhabditis elegans*, UNC-86 (the Pou4f3 homolog) is required for the generation and the differentiation of touch neurons (43,44). UNC-86 promotes touch neuron differentiation via the activation of *mec-3*, and a synergistic activation of transcription of touch neuron specific genes with the protein product of *mec-3* (45–47). UNC-86 and MEC-3 function together to activate *mec-7* transcription, a gene that is necessary for the function of touch cells (45). The onset of *Pag-3* expression (the *Gfi1* homolog) in the touch receptor neurons parallels that of *mec-7* (48,49), suggesting an evolutionary conserved transcriptional cascade in the mouse and *C. elegans.* This is supported by our finding that *Gfi1* mRNA co-localizes with and follows the expression pattern of Pou4f3, and that Gfi1 expression is significantly reduced or absent in *Pou4f3* loss of function mutants. Consistent with this hypothesis is the recent report that retinas from *Pou4f2*$^{-/-}$ mice lack expression of *Gfi1*$^{-/-}$, indicating that multiple class IV POU domain transcription factors may function upstream of *Gfi1* (50).

Our results demonstrate that a transcription profiling experimental strategy, starting with inner ears of embryonic mice, can reveal gene expression changes that are specific for hair cells. This approach was expected to result in the identification

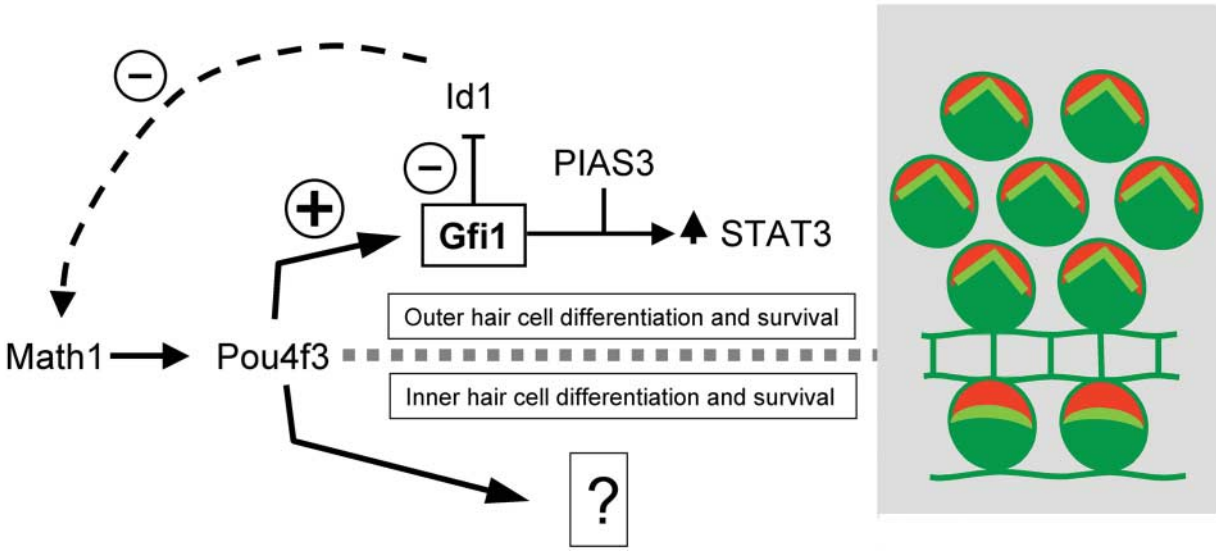

Figure 6. A working model of the transcriptional cascade leading to Pou4f3/Gfi1 regulation of cochlear hair cell survival. The transcription factor Math1 is necessary and sufficient to induce all hair cells formation in the inner ear. Pou4f3 is the first transcription factor shown to be expressed in all hair cells of the cochlear epithelium as soon as they exit the cell cycle and assume a hair cell fate. Increased Pou4f3 levels positively regulate outer hair cells survival and differentiation through the regulation of Gfi1, another transcription factor. Gfi1 may act through a PIAS3/STAT3 cascade, but could also inhibit Id1 expression, which could downregulate Math1 expression. The downstream targets of Pou4f3 in the inner hair cells are not known, and seem to differ from those of the outer hair cells.

of bona fide Pou4f3 target genes, as we assumed at least some of the downstream effectors of Pou4f3 will also be hair cell specific molecules. Moreover, previous reports suggested that there may be remarkably large differences between the results of gene regulation of class IV POU domain proteins *in vivo* and *in vitro* (51,52).

While hair cell differentiation and survival is dependent on a multitude of genes, the identification of Gfi1 as an effector gene of Pou4f3 sheds light on a pathway that is involved in hair cell differentiation and survival (Fig. 6). We believe that with the multitude of deafness genes and mouse models that are available, our approach could be successfully applied to elucidate the underlying molecular pathogenesis of many additional forms of deafness, eventually leading to the development of general or gene-specific therapies for hearing loss.

MATERIALS AND METHODS

Breeding, phenotyping and genotyping of mice

All procedures involving animals met the guidelines described in the National Institutes of Health Guide for the Care and Use of Laboratory Animals and had been approved previously by the Animal Care and Use Committees of The Jackson Laboratory, the National Institutes of Health, and Tel Aviv University (M-00-65). All lines were maintained by crossing heterozygotes. To generate homozygous embryos, pregnant females were euthanized at the desired gestational stage. The appearance of a copulation plug was considered embryonic day 0.5. A definitive determination of the developmental stage of each embryo at the time of harvesting was based on Theiler stages (53). ABR thresholds were measured at 32 weeks of age with clicks and 8, 16 and 32 kHz tone bursts, and auditory thresholds (dB SPL) were obtained for each stimulus as described previously (54).

In dreidel (*Pou4f3*$^{ddl/ddl}$) mice, *Pou4f3* was sequenced and a dinucleotide TG deletion (388del2), which omits a *Blp*I restriction endonuclease recognition site at nucleotides 841–842 of the *Pou4f3* sequence, was identified (GenBank accession number S69352). Primers were designed to amplify the genomic sequence surrounding this deletion and a *Blp*I restriction digestion was performed to differentiate between the wild-type and mutant alleles: ddl-645 (F) 5′-GCGGTGGATA TCGTCTC-3′ and ddl-1165 (R) 5′-GTAAGAGACTCGAACC TGC-3′. *Pou4f3*$^{-/-}$ knockout mice were a gift from Mengqing Xiang (UMDNJ–Robert Wood Johnson Medical School, NJ, USA) (8). Genotyping was performed by a multiplex PCR reaction using the following primers: MX176, 5′-TGATGCCGCCG TGTTCCGGCTGT-3′; MX177, 5′-TCGCCGCCAAGCTCTTC AGCAAT-3′ MX183 5′-CCTCTCCTCAAAGCCCAGGTCA T-3′ and MX226 5′-CCCTGCCAGACTCCCGAAGAT-3′. The expected PCR product sizes are 600 bp for the neomycin cassette (MX176 + MX177) and 400 bp for the wild-type *Pou4f3* allele (MX183 + MX226). *Gfi1*$^{-/-}$ knockout mice were genotyped as described (20) using the following primers: mgfi2 5′-GTAGGTTTGCTGAACTGCTGTG-3′; mgfi3 5′-GCTATC TAACCGCTAAACTG-3′ and PB3 5′-CTTCCATTTGTCAC GTCCTG-3′. The expected product sizes are 320 bp for the *Gfi1* knockout allele and 220 bp for the wild-type allele.

RNA extraction and reverse transcription

For microarray analysis and validation of differential gene expression, total RNA was extracted from whole inner ears isolated at E16.5 and E18.5 from wild-type, *Pou4f3*$^{ddl/ddl}$ and *Pou4f3*$^{-/-}$ mice. Total RNA was prepared from 4 to 10

inner ears per 1 ml of TRIzol (Invitrogen Life Technologies), DNA was removed with DNA-Free (Ambion), and RNA was twice purified with PCI (PCI; Invitrogen) Reverse transcription (RT) reactions were performed by using the SuperScript™ First-Strand Synthesis System for RT–PCR (Invitrogen) with oligo(dT) priming.

For developmental semi-quantitative profiling of mRNA abundance, mouse auditory sensory epithelia were isolated from embryos of timed mated ICR females and separated from the underlying mesenchyme as previously described (22). RNA was then extracted using the StrataPrep Total RNA Miniprep Kit (Stratagene).

Affymetrix oligonucleotide microarrays

RNA was extracted from inner ears of E16.5 *Pou4f3*$^{ddl/ddl}$ mutants and their wild-type littermate controls as described. The microarray experiment was performed in independent triplicates and each RNA pool consisted of four inner ears from mice of the same genotype. Ten micrograms of total RNA was processed and hybridized to the murine genome U74Av2 oligonucleotide arrays (Affymetrix), containing probe sets for the detection of over 12 000 cDNAs, following the manufacturer's protocol. Each hybridization cocktail was hybridized to another microarray as internal repeat. Scanned output files were visually inspected for hybridization artifacts and analyzed using MAS 5.0 software (Affymetrix). Arrays were scaled to an average intensity of 150. Each expression level computed by the Affymetrix software is accompanied by a presence flag (A, absent; P, present; M, marginal), indicating the authenticity of the gene's recorded expression level, on the basis of a comparison between signals obtained from its perfect-match and mismatch probes (55). In order to identify genes that were expressed differentially between the two genotypes, we employed a statistical *t*-test analysis. Before applying the test, intensity levels below 20 were set to 20 (to reduce identification of changes at the noise level), and then intensity values were log-transformed. The full dataset can be downloaded as an Excel file (Supplementary Material, Table S1).

Real-time RT–PCR

Real-time multiplex RT–PCR reactions were performed in triplicate for the developmental expression pattern series, and six repeats for the validation PCRs using an ABI Prism 7700 Sequence Detector (PE Applied Biosystems), VIC labeled *Gapdh* control primers (150 nM) and probe (PE Applied Biosystems) and the following primers (600 nM) and FAM labeled probes (PE Applied Biosystems): *Myo6* (F) 5′-CA TTTTGACGGACCCTGGATT-3′, (R) 5′-TTGTAGCTG GC AAGGATGACAT-3′, (probe) 6FAM-TGCACCCTGACA AGCCACCCATC-TAMRA; *Myo7a* (F) 5′-AACTGGAGTA GTGGCAACACCTACT-3′, (R) 5′-GCGATGTCTCACAGA GCAGTTT-3′, (probe) 6FAM-CCACATCACCATTGGGAA CTTGGTCC-TAMRA; *Pou4f3* (F) 5′-GGCATGCACCCCG TACTG-3′, (R) 5′-GGCGCATGGCCTCAGA-3′, (probe) 6FAM-AACCCAAATTCTCCAGCCTACACTCCGG-TAM RA; *Gfi1* (F) 5′-AGCTGTGTAACACTACCGTGAGGAT-3′, (R) 5′-ACCATGATGAGCTTTGCACACT-3′, (probe) 6FAM-TTCCCTGCCTCCCTCCAGCCC-TAMRA. For *Math1*, the *Gapdh* control primers were used at 75 nM with the following primers and probe: (F) 5′-AAGCAAA GGAGGCTGGCAG-3′ (300 nM), (R) 5′-TGGTTCAGCCCGTGCAT-3′ (600 nM), (probe) 6FAM-AAACGCAAGGGAAC GGCGCA-TAMRA.

In situ hybridization

A 484 bp segment of the unique coding sequence of the *Pou4f3* gene (NM_138945, nucleotides 13–496) and a 958 bp segment of the 3′ untranslated region of the *Gfi1* gene (NM_010278, nucleotides 1781–2738) were cloned into the pGEM-T Easy Vector (Promega) for the generation of digoxigenin labeled sense and antisense probes. Whole mount *in situ* hybridization to detect *Pou4f3* and *Gfi1* mRNA were performed on cochlea of E16.5, E18.5 and P0 wild-type mice and E18.5 *Pou4f3*$^{ddl/ddl}$ mice and their wild-type littermate controls, as previously described, with modifications (56). *Pou4f3* and *Gfi1 in situ* hybridization were also performed on 12 μm cryostat sections of whole inner ears of E18.5 *Pou4f3*$^{ddl/ddl}$ and wild-type littermate controls as previously described (57). All experiments were repeated at least three times with mice from at least three separate litters.

Immunohistochemistry, peroxidase immunostaining and immunofluorescence

After fixation in 4% paraformaldehyde, samples were rinsed in phosphate buffered saline (PBS), and incubated in 10% normal goat serum in PBS with 0.5% Tween-20 (PBS-T). The samples were then incubated with primary antibodies. Binding of the primary antibody was detected by immunofluorescence or peroxidase immunostaining. Samples that were detected by peroxidase immunostaining were incubated in a 0.3–0.6% H_2O_2 solution in PBS-T, prior to the incubation with goat serum. For peroxidase immunostaining, after incubation with a myosin VI antibody (obtained from Tama Hasson), an affinity purified Pou4f3 antibody (Covance; for affinity purification, AminoLink Kit) or a STAT3 antibody (Cell Signaling), the samples were rinsed and incubated with a biotin-conjugated secondary antibody (Jackson ImmunoResearch Labs). The samples were then reacted with diaminobenzidine using an Elite ABC kit (Vector Laboratories) with nickel intensification. For immunofluorescence, after incubation with an antibody specific for p75^{ntr} (Chemicon), or the Pou4f3 antibody, samples were rinsed, and incubated with an Alexa Fluor 594 (red) or 488 (green)-conjugated secondary antibodies (Molecular Probes). Following antibody labeling, filamentous actin was labeled in the same samples by incubating with Alexa Fluor 488 or 594-conjugated phalloidin (Molecular Probes). Samples were then mounted in anti-fade medium (Slowfade Antifade kit; Molecular Probes), and observed using a Zeiss LSM510 confocal microscope. For GFP immunolocalization, the cochleae were incubated with an Alexa Fluor 488-conjugated GFP antibody (Molecular Probes) and Alexa Fluor 594-conjugated phalloidin (Molecular Probes).

Scanning electron microscopy

SEM was performed on cochleae of *Pou4f3*$^{-/-}$, *Gfi1*$^{-/-}$ and their heterozygous and wild-type littermates at E18.5 and P0, as previously described (58) using a JEOL JSM 6400 scanning electron microscope. The experiment was performed on at least four inner ears for each mutant at E18.5 and P0.

SUPPLEMENTARY MATERIAL

Supplementary Material is available at HMG Online.

ACKNOWLEDGEMENTS

We thank Leeat Anker, Kip Bartlett, Alain Dabdoub, Tama Hasson, Bonnie Jacques, Jennifer Jones, Robert Morell, Tama Sobe, Mengqing Xiang and Qing Yin Zheng for experimental advice and reagents, and Dennis Drayna, Sadaf Naz, Susan Sullivan and Robert Wenthold for critical reading of the manuscript. This research was supported by funds from the Israel Science Foundation—The Dorot Science Fellowships Foundation (grant no. 740/01) (K.B.A.), NIH grant R01 DC005641 (K.B.A.), National Institute of Deafness and Other Communication Disorders, NIH Intramural support DC000039-07 (T.B.F.) and DC000059-04 (M.W.K.), NIH grant DC03611 (W.N.F.), NIH grant DC04376 (Qing Yin Zhang), the Deutsche Forschungsgemeinschaft, DFG (grant no. 435/10–4, 10–5), the 'Fonds der chemischen Industrie', the European Community Framework 5 Program, the 'IFORES Program' of the University of Essen-Duisburg Medical School (T.M.), and the TAU–NIH Program for Israeli Predoctoral Biomedical Researchers (R.H.). This work was performed in the partial fulfillment of the requirements for an MD–PhD degree of R.H., Faculty of Medicine, Tel Aviv University, Israel.

REFERENCES

1. Gaffney, M., Gamble, M., Costa, P., Holstrum, J. and Boyle, C. (2003) Infants tested for hearing loss—United States, 1999–2001. *JAMA*, **52**, 981–984.
2. Friedman, T.B. and Griffith, A.J. (2003) Human nonsyndromic sensorineural deafness. *Annu. Rev. Genomics Hum. Genet.*, **4**, 341–402.
3. Petit, C., Levilliers, J. and Hardelin, J.P. (2001) Molecular genetics of hearing loss. *Annu. Rev. Genet.*, **35**, 589–646.
4. Vahava, O., Morell, R., Lynch, E.D., Weiss, S., Kagan, M.E., Ahituv, N., Morrow, J.E., Lee, M.K., Skvorak, A.B., Morton, C.C. *et al.* (1998) Mutation in transcription factor *POU4F3* associated with inherited progressive hearing loss in humans. *Science*, **279**, 1950–1954.
5. Weiss, S., Gottfried, I., Mayrose, I., Khare, S.L., Xiang, M., Dawson, S.J. and Avraham, K.B. (2003) The DFNA15 deafness mutation affects POU4F3 protein stability, localization, and transcriptional activity. *Mol. Cell. Biol.*, **23**, 7957–7964.
6. Erkman, L., McEvilly, R.J., Luo, L., Ryan, A.K., Hooshmand, F., O'Connell, S.M., Keithley, E.M., Rapaport, D.H., Ryan, A.F. and Rosenfeld, M.G. (1996) Role of transcription factors Brn-3.1 and Brn-3.2 in auditory and visual system development. *Nature*, **381**, 603–606.
7. Wang, S.W., Mu, X., Bowers, W.J., Kim, D.S., Plas, D.J., Crair, M.C., Federoff, H.J., Gan, L. and Klein, W.H. (2002) Brn3b/Brn3c double knockout mice reveal an unsuspected role for Brn3c in retinal ganglion cell axon outgrowth. *Development*, **129**, 467–477.
8. Xiang, M., Gan, L., Li, D., Chen, Z.Y., Zhou, L., O'Malley, B.W., Jr, Klein, W. and Nathans, J. (1997) Essential role of POU-domain factor Brn-3c in auditory and vestibular hair cell development. *Proc. Natl Acad. Sci. USA*, **94**, 9445–9450.
9. Gillespie, P.G. and Walker, R.G. (2001) Molecular basis of mechanosensory transduction. *Nature*, **413**, 194–202.
10. Gan, L., Xiang, M., Zhou, L., Wagner, D.S., Klein, W.H. and Nathans, J. (1996) POU domain factor Brn-3b is required for the development of a large set of retinal ganglion cells. *Proc. Natl Acad. Sci. USA*, **93**, 3920–3925.
11. Xiang, M., Gan, L., Zhou, L., Klein, W.H. and Nathans, J. (1996) Targeted deletion of the mouse POU domain gene Brn-3a causes selective loss of neurons in the brainstem and trigeminal ganglion, uncoordinated limb movement, and impaired suckling. *Proc. Natl Acad. Sci. USA*, **93**, 11950–11955.
12. McEvilly, R.J., Erkman, L., Luo, L., Sawchenko, P.E., Ryan, A.F. and Rosenfeld, M.G. (1996) Requirement for Brn-3.0 in differentiation and survival of sensory and motor neurons. *Nature*, **384**, 574–577.
13. Xiang, M., Gao, W.-Q., Hasson, T. and Shin, J.J. (1998) Requirement for Brn-3c in maturation and survival, but not in fate determination of inner ear hair cells. *Development*, **125**, 3935–3946.
14. Ruben, R.J. (1967) Development of the inner ear of the mouse: a radioautographic study of terminal mitoses. *Acta Otolaryngol. Suppl.*, **220**, 1–44.
15. Xiang, M., Maklad, A., Pirvola, U. and Fritzsch, B. (2003) Brn3c null mutant mice show long-term, incomplete retention of some afferent inner ear innervation. *BMC Neurosci.*, **4**, 2.
16. Bermingham, N.A., Hassan, B.A., Price, S.D., Vollrath, M.A., Ben-Arie, N., Eatock, R.A., Bellen, H.J., Lysakowski, A. and Zoghbi, H.Y. (1999) Math1: an essential gene for the generation of inner ear hair cells. *Science*, **284**, 1837–1841.
17. Li, S., Price, S.M., Cahill, H., Ryugo, D.K., Shen, M.M. and Xiang, M. (2002) Hearing loss caused by progressive degeneration of cochlear hair cells in mice deficient for the *Barhl1* homeobox gene. *Development*, **129**, 3523–3532.
18. Wallis, D., Hamblen, M., Zhou, Y., Venken, K.J., Schumacher, A., Grimes, H.L., Zoghbi, H.Y., Orkin, S.H. and Bellen, H.J. (2003) The zinc finger transcription factor Gfi1, implicated in lymphomagenesis, is required for inner ear hair cell differentiation and survival. *Development*, **130**, 221–232.
19. Hock, H., Hamblen, M.J., Rooke, H.M., Traver, D., Bronson, R.T., Cameron, S. and Orkin, S.H. (2003) Intrinsic requirement for zinc finger transcription factor Gfi-1 in neutrophil differentiation. *Immunity*, **18**, 109–120.
20. Karsunky, H., Zeng, H., Schmidt, T., Zevnik, B., Kluge, R., Schmid, K.W., Duhrsen, U. and Möröy, T. (2002) Inflammatory reactions and severe neutropenia in mice lacking the transcriptional repressor Gfi1. *Nat. Genet.*, **30**, 295–300.
21. Chen, Z.Y. and Corey, D.P. (2002) An inner ear gene expression database. *J. Assoc. Res. Otolaryngol.*, **3**, 140–148.
22. Montcouquiol, M. and Corwin, J.T. (2001) Intracellular signals that control cell proliferation in mammalian balance epithelia: key roles for phosphatidylinositol-3 kinase, mammalian target of rapamycin, and S6 kinases in preference to calcium, protein kinase C, and mitogen-activated protein kinase. *J. Neurosci.*, **21**, 570–580.
23. Yücel, R., Kosan, C., Heyd, F. and Möröy, T. (2004) Gfi1 : Gfp knock-in mutant reveals differential expression and auto-regulation of the gene *growth factor independence 1* (*Gfi1*) during lymphocyte development. *J. Biol. Chem.*, in press (epub ahead of print).
24. von Bartheld, C.S., Patterson, S.L., Heuer, J.G., Wheeler, E.F., Bothwell, M. and Rubel, E.W. (1991) Expression of nerve growth factor (NGF) receptors in the developing inner ear of chick and rat. *Development*, **113**, 455–470.
25. Anniko, M. (1983) Cytodifferentiation of cochlear hair cells. *Am. J. Otolaryngol.*, **4**, 375–388.
26. Lim, D.J. and Anniko, M. (1985) Developmental morphology of the mouse inner ear. A scanning electron microscopic observation. *Acta Otolaryngol. Suppl.*, **422**, 1–69.
27. Rödel, B., Tavassoli, K., Karsunky, H., Schmidt, T., Bachmann, M., Schaper, F., Heinrich, P., Shuai, K., Elsasser, H.P. and Möröy, T. (2000) The zinc finger protein Gfi-1 can enhance STAT3 signaling by interacting with the STAT3 inhibitor PIAS3. *EMBO J.*, **19**, 5845–5855.
28. Alonzi, T., Middleton, G., Wyatt, S., Buchman, V., Betz, U.A., Muller, W., Musiani, P., Poli, V. and Davies, A.M. (2001) Role of STAT3

and PI 3-kinase/Akt in mediating the survival actions of cytokines on sensory neurons. *Mol. Cell. Neurosci.*, **18**, 270–282.
29. Catlett-Falcone, R., Landowski, T.H., Oshiro, M.M., Turkson, J., Levitzki, A., Savino, R., Ciliberto, G., Moscinski, L., Fernandez-Luna, J.L., Nunez, G. *et al.* (1999) Constitutive activation of Stat3 signaling confers resistance to apoptosis in human U266 myeloma cells. *Immunity*, **10**, 105–115.
30. Fukada, T., Hibi, M., Yamanaka, Y., Takahashi-Tezuka, M., Fujitani, Y., Yamaguchi, T., Nakajima, K. and Hirano, T. (1996) Two signals are necessary for cell proliferation induced by a cytokine receptor gp130: involvement of STAT3 in anti-apoptosis. *Immunity*, **5**, 449–460.
31. Grimes, H.L., Chan, T.O., Zweidler-McKay, P.A., Tong, B. and Tsichlis, P.N. (1996) The Gfi-1 proto-oncoprotein contains a novel transcriptional repressor domain, SNAG, and inhibits G1 arrest induced by interleukin-2 withdrawal. *Mol. Cell. Biol.*, **16**, 6263–6272.
32. Zweidler-Mckay, P.A., Grimes, H.L., Flubacher, M.M. and Tsichlis, P.N. (1996) Gfi-1 encodes a nuclear zinc finger protein that binds DNA and functions as a transcriptional repressor. *Mol. Cell. Biol.*, **16**, 4024–4034.
33. McGhee, L., Bryan, J., Elliott, L., Grimes, H.L., Kazanjian, A., Davis, J.N. and Meyers, S. (2003) Gfi-1 attaches to the nuclear matrix, associates with ETO (MTG8) and histone deacetylase proteins, and represses transcription using a TSA-sensitive mechanism. *J. Cell. Biochem.*, **89**, 1005–1018.
34. Duan, Z. and Horwitz, M. (2003) Targets of the transcriptional repressor oncoprotein Gfi-1. *Proc. Natl Acad. Sci. USA*, **100**, 5932–5937.
35. Gilks, C.B., Bear, S.E., Grimes, H.L. and Tsichlis, P.N. (1993) Progression of interleukin-2 (IL-2)-dependent rat T cell lymphoma lines to IL-2-independent growth following activation of a gene (Gfi-1) encoding a novel zinc finger protein. *Mol. Cell. Biol.*, **13**, 1759–1768.
36. Zhu, J., Guo, L., Min, B., Watson, C.J., Hu-Li, J., Young, H.A., Tsichlis, P.N. and Paul, W.E. (2002) Growth factor independent-1 induced by IL-4 regulates Th2 cell proliferation. *Immunity*, **16**, 733–744.
37. Zörnig, M., Schmidt, T., Karsunky, H., Grzeschiczek, A. and Möröy, T. (1996) Zinc finger protein GFI-1 cooperates with myc and pim-1 in T-cell lymphomagenesis by reducing the requirements for IL-2. *Oncogene*, **12**, 1789–1801.
38. Yücel, R., Karsunky, H., Klein-Hitpass, L. and Möröy, T. (2003) The transcriptional repressor Gfi1 affects development of early, uncommitted c-Kit+ T cell progenitors and CD4/CD8 lineage decision in the thymus. *J. Exp. Med.*, **197**, 831–844.
39. Jen, Y., Manova, K. and Benezra, R. (1997) Each member of the Id gene family exhibits a unique expression pattern in mouse gastrulation and neurogenesis. *Dev. Dyn.*, **208**, 92–106.
40. Sikder, H.A., Devlin, M.K., Dunlap, S., Ryu, B. and Alani, R.M. (2003) Id proteins in cell growth and tumorigenesis. *Cancer Cell*, **3**, 525–530.
41. Ben-Arie, N., McCall, A.E., Berkman, S., Eichele, G., Bellen, H.J. and Zoghbi, H.Y. (1996) Evolutionary conservation of sequence and expression of the bHLH protein Atonal suggests a conserved role in neurogenesis. *Hum. Mol. Genet.*, **5**, 1207–1216.
42. Nolo, R., Abbott, L.A. and Bellen, H.J. (2000) Senseless, a Zn finger transcription factor, is necessary and sufficient for sensory organ development in *Drosophila. Cell*, **102**, 349–362.
43. Chalfie, M., Horvitz, H.R. and Sulston, J.E. (1981) Mutations that lead to reiterations in the cell lineages of *C. elegans. Cell*, **24**, 59–69.
44. Ninkina, N.N., Stevens, G.E., Wood, J.N. and Richardson, W.D. (1993) A novel Brn3-like POU transcription factor expressed in subsets of rat sensory and spinal cord neurons. *Nucl. Acids Res.*, **21**, 3175–3182.
45. Duggan, A., Ma, C. and Chalfie, M. (1998) Regulation of touch receptor differentiation by the *Caenorhabditis elegan*s mec-3 and unc-86 genes. *Development*, **125**, 4107–4119.
46. Lichtsteiner, S. and Tjian, R. (1995) Synergistic activation of transcription by UNC-86 and MEC-3 in *Caenorhabditis elegans* embryo extracts. *EMBO J.*, **14**, 3937–3945.
47. Rohrig, S., Rockelein, I., Donhauser, R. and Baumeister, R. (2000) Protein interaction surface of the POU transcription factor UNC-86 selectively used in touch neurons. *EMBO J.*, **19**, 3694–3703.
48. Sze, J.Y., Liu, Y. and Ruvkun, G. (1997) VP16-activation of the *C. elegans* neural specification transcription factor UNC-86 suppresses mutations in downstream genes and causes defects in neural migration and axon outgrowth. *Development*, **124**, 1159–1168.
49. Jia, Y., Xie, G., McDermott, J.B. and Aamodt, E. (1997) The *C. elegans* gene pag-3 is homologous to the zinc finger proto-oncogene gfi-1. *Development*, **124**, 2063–2073.
50. Yang, Z., Ding, K., Pan, L., Deng, M. and Gan, L. (2003) Math5 determines the competence state of retinal ganglion cell progenitors. *Dev. Biol.*, **264**, 240–254.
51. Eng, S.R., Kozlov, S. and Turner, E.E. (2003) Unaltered expression of Bcl-2 and TAG-1/axonin-1 precedes sensory apoptosis in Brn3a knockout mice. *Neuroreport*, **14**, 173–176.
52. Trieu, M., Ma, A., Eng, S.R., Fedtsova, N. and Turner, E.E. (2003) Direct autoregulation and gene dosage compensation by POU-domain transcription factor Brn3a. *Development*, **130**, 111–121.
53. Kaufman, M.H. (1995) *The Atlas of Mouse Development*. Academic Press, London.
54. Zheng, Q.Y., Johnson, K.R. and Erway, L.C. (1999) Assessment of hearing in 80 inbred strains of mice by ABR threshold analyses. *Hear. Res.*, **130**, 94–107.
55. Lipshutz, R.J., Fodor, S.P., Gingeras, T.R. and Lockhart, D.J. (1999) High density synthetic oligonucleotide arrays. *Nat. Genet.*, **21**, 20–24.
56. Lanford, P.J., Shailam, R., Norton, C.R., Gridley, T. and Kelley, M.W. (2000) Expression of Math1 and HES5 in the cochleae of wildtype and Jag2 mutant mice. *J. Assoc. Res. Otolaryngol.*, **1**, 161–171.
57. Wu, D.K. and Oh, S.H. (1996) Sensory organ generation in the chick inner ear. *J. Neurosci.*, **16**, 6454–6462.
58. Self, T., Sobe, T., Copeland, N.G., Jenkins, N.A., Avraham, K.B. and Steel, K.P. (1999) Role of myosin VI in the differentiation of cochlear hair cells. *Dev. Biol.*, **214**, 331–341.